Improving Brain MRI Image Segmentation Quality: A Hybrid Technique for Intensity Inhomogeneity Correction

Samah Abdel Aziz*, Ammar Hawbani*‖, Xingfu Wang*‖, Talaat Abdelhamid‡, Ismail Y. Maolood§,Saeed Alsamhi¶, A. S. Ismail*
*School of Computer Science and Technology, University of Science and Technology of China, Hefei, 23002, China
†Zagazig University, Zagazig, 44519, Egypt
‡ Faculty of Electronic Engineering, Menoufia University Menoufia, Egypt
§Information and Communication Technology Center (ICTC)-System Information, Ministry of Higher Education and Scientific Research, Erbil, Kurdistan Region, Iraq
¶Insight Centre for Data Analytics, National University of Ireland, Galway, Ireland
samahhabib10@yahoo.com, anmande@ustc.edu.cn, wangxfu@ustc.edu.cn,Talaat_abdelhamid@el-eng.menofia.edu.eg, ismail.maulood@mhe-krg.org,saeed.alsamhi@insight-centre.org, a.sami@zu.edu.eg
‖Corresponding authors: Ammar Hawbani, Xingfu Wang

***Abstract*—Intensity inhomogeneity is a significant issue in magnetic resonance imaging (MRI), where the presence of bias field causes distortions in pixel values, resulting in inconsistent and erroneous intensities across the image. This artifact not only hampers accurate diagnosis by radiologists but also negatively impacts the performance of computer-aided diagnosis algorithms, particularly in tasks like segmentation. In our proposed approach, we use a hybrid technique called KIFCM, which integrates K-means and Fuzzy C-means to enhance brain tumor segmentation. K-means provides computational efficiency, while Fuzzy C-means improves accuracy by detecting missed tumor cells. We employ a bias correction method based on the level set framework, removing noise with a median filter and applying the hybrid KIFCM technique for optimal segmentation. Our method effectively addresses intensity variation challenges, ensuring precise brain tumor region segmentation. We compare our results with DFCM and MFFLs, and the comparison shows the efficiency of our proposed method by highlighting the superior quality and accuracy of 81% achieved, requiring less computational time. Consequently, our results demonstrate KIFCM's potential to boost both accuracy and speed in MRI-based brain tumor detection through computer-aided diagnosis.**

I. Introduction

Brain tumors pose significant challenges in their recognition and detection due to the complexity of the brain structure. The use of medical imaging devices is vital in delivering a vast amount of anatomical and functional data, resulting in improved diagnosis and patient care, particularly when coupled with quantitative image analysis methods [1]. MRI is widely recognized as a reliable modality for brain tumor diagnosis, providing high-resolution and multiplanar imaging capabilities that aid in tumor detection, localization, and characterization [2], [3].

However, accurate segmentation of brain tumors from medical images, especially MRI, is crucial for diagnosis and treatment planning [4]. The presence of artifacts, such as noise, poor image quality, and intensity inhomogeneity, hinders the effectiveness of tumor segmentation algorithms. Therefore, addressing intensity inhomogeneity is essential for accurate image analysis [5].

Image acquisition serves as the initial step in determining brain tumor diagnoses, consisting of modalities, patient data, and software processed through mathematical operations to accurately identify the entire pathological organ. Segmentation, which plays a pivotal role in the medical image processing pipeline, involves identifying, analyzing, detecting, and recognizing irregular regions within medical images [6]. It is an essential step in facilitating accurate diagnosis and treatment decision-making [7]. Numerous studies have focused on solving the challenges associated with brain tumor segmentation using MRI modality [8], [1], [9], [10], [11].

Intensity inhomogeneity in MRI is a common issue that hampers the accuracy of quantitative image analysis. It arises from factors during image acquisition, causing variations in luminance quality and imperfections in imaging devices. This inhomogeneity complicates the precise identification of tumor areas based on pixel values, especially when overlapping intensity ranges occur between regions to be segmented. The undesired smooth and varying bias field in MRI introduces pixel inconsistencies within the same tissue, leading to reduced tissue contrast and affecting interpretation [12]. This has significant implications, particularly in conditions involving white matter diseases, where intensity symmetry is crucial. The bias field's variation in true pixel intensity causes semantic inconsistencies, adversely impacting tasks like computer-aided diagnosis and image processing algorithms such as segmentation and registration.

The mathematical representation of the intensity inhomo-

geneity artifact is expressed as in Eq.(1):

$$v(x,y) = u(x,y) \cdot b(x,y) + n(x,y) \quad (1)$$

where, $v(x,y)$ represents the intensity inhomogeneity-corrupted image, $u(x,y)$ represents the intensity inhomogeneity-free image, $b(x,y)$ represents the bias field, and $n(x,y)$ represents the noise component. Unfortunately, MRI images often suffer from issues such as intensity inhomogeneity or nonuniformity, which arise from imperfect image acquisition systems. Traditional segmentation methods solely rely on spatial information of pixel intensities, making them vulnerable to noise, intensity inhomogeneity (IIH), and intensity nonuniformity (INU). To overcome these challenges, The authors in [13] proposed a novel approach that leveraged the fusion of multiple Gaussian surfaces to estimate and correct INU in MRI brain images. Subsequently, the corrected images underwent segmentation using a probabilistic fuzzy c-means (FCM) algorithm, which combines both spatial features and intensity corrections to achieve more accurate and robust segmentation results.

To address the challenge of varying intensities caused by different scanners and acquisition protocols, correcting the magnetic field bias is crucial. This bias correction step is of major importance in subsequent medical image analysis, and this paper focuses on discussing this aspect as a key solution to overcome the challenge. We present a novel contribution in the field of brain tumor segmentation as follows:

- Using a hybrid technique called K-means integrated with Fuzzy C-means (KIFCM). Our approach aims to overcome limitations by combining the strengths of both techniques. K-means clustering offers computational efficiency and faster processing for detecting and identifying brain tumors. On the other hand, Fuzzy C-means provides higher accuracy by effectively identifying tumor cells that may be missed by K-means alone.
- To further enhance the accuracy of segmentation, we propose a bias correction method based on the level set framework. Our proposed method begins by removing noise using a median filter, followed by the application of the hybrid KIFCM technique. This enables us to achieve optimal segmentation results with a reduced number of iterations and low computational time.
- Additionally, we address the challenge of intensity variation between regions to be segmented by employing bias correction based on the level set. This approach effectively mitigates the impact of intensity variations, ensuring accurate segmentation of brain tumor regions.

Finally, the rest of this paper is organized as follows. Section II introduces the methodology, which includes image acquisition, median filtering, clustering algorithm, and level set method as subsections. In Section III, results and analysis are discussed as tech-driven urban green spaces exploration. Section IV presents the evaluation metrics. Finally, a conclusion for this paper is offered.

II. Methodology

Our research presents a novel method to tackle the issue of intensity inhomogeneity in brain MRI image segmentation. Our proposed method is shown in Fig. 1. To address the presence of noise artifacts, we implemented the Median filter [14], a nonlinear filtering technique. We aimed to harness the strengths of both Fuzzy C-means and K-means clustering methods by employing a combined approach called the K-means integrated with Fuzzy C-means (KIFCM) algorithm. The selection of these algorithms was driven by their computational efficiency in segmenting the images.

To ensure accurate segmentation despite intensity inhomogeneity, we utilized the level set framework. This framework enabled us to assess the contour beyond the image boundaries and subsequently apply bias correction. By integrating these components, our objective was to specifically address the challenge of segmenting images with intensity inhomogeneity, while considering important factors such as computational time, iteration count, and segmentation accuracy.

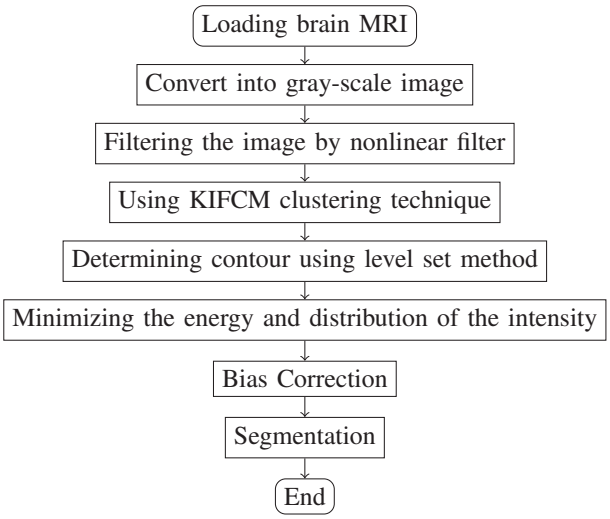

Fig. 1. Our proposed method

A. Image Acquisition

In this part, we applied the proposed Method on a brain MRI image dataset obtained from the website (http://www.med.harvard.edu/AANLIB/home.html). The dataset consists of approximately 60 images. For the experiments, we generated the dataset by varying the parameter σ within the range of $4 \leq \sigma \leq 7$ for all the images.

B. Median Filtering

Median filtering is a technique utilized for removing noise and preserving edges in images. Several studies have provided evidence supporting the superiority of median filtering over linear filtering when it comes to noise removal in processed images [15]. It operates by examining each pixel in the image and replacing its value with the median value derived from its neighboring pixels. The process commences with the

arrangement of all pixel values within a designated window into a numerical sequence. Subsequently, the pixel values are substituted with the middle value of this sorted sequence. Multiple steps are involved in determining the median value. Initially, the pixel value to be processed, in conjunction with its neighboring pixels, is read. Next, the pixel values are sorted in ascending order. Ultimately, the value situated in the middle of the sorted sequence is chosen as the new value for the pixel (x, y) which is represented as follows in Eq.(2).

$$y[m, n] = \text{median}\,\{x[i, j] \,|\, [i, j] \in \Omega\} \tag{2}$$

where, $y[m, n]$ represents the filtered output pixel at location (m, n) in the image. The median operator, denoted by median, is applied to the set of pixel values $x[i, j]$ within a neighborhood defined by Ω. The neighborhood is represented by the set of indices $[i, j]$ that satisfy $[i, j] \in \Omega$.

By taking the median value of the pixel values within the specified neighborhood, the median filter replaces the target pixel at (m, n) with a value that is less affected by noise and outliers, resulting in noise reduction in the filtered image. In our work, to obtain the filtered image using the Median filter, we divided the image into blocks of size 3×3 and sorted the pixel values in ascending order. Subsequently, we selected the middle value as the target pixel and replaced the original pixel with this value. This process of sorting, selecting, and changing the target pixel with the middle value was repeated until the entire image was covered.

By applying this approach, we aimed to mitigate the effects of noise and enhance the quality of the images in our dataset. The utilization of the Median filter within a block-based framework allowed for effective noise reduction, contributing to improved image clarity and subsequent analysis. The result of the median filtering can be observed in Fig. 2, where the blurring effect is evident. And Algorithm 1 shows how the median filter works to obtain filtered brain MRI images.

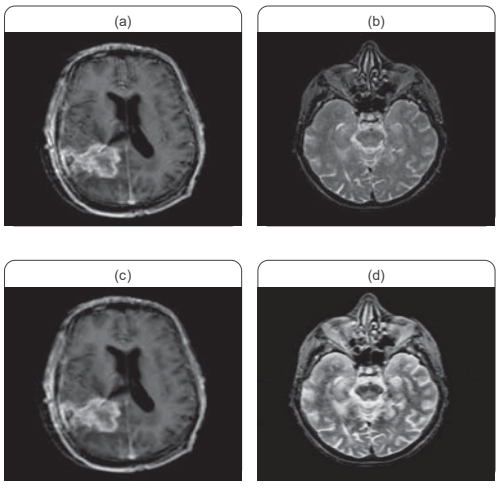

Fig. 2. (a and b) are original brain MRI images and (c and d) are filtered images respectively

Algorithm 1 Median Filter Algorithm

Require: Brain MRI image
Ensure: Filtered brain MRI image by median filter
1: Read the brain MRI image.
2: Divide the image into blocks of size 3×3.
3: **for** each block in the image **do**
4: Sort the values of pixels in ascending order.
5: Choose the middle value.
6: Change the target pixel with the middle value.
7: **end for**
8: **return** filtered brain MRI image

C. Clustering Algorithm

An automated and precise clustering technique for MRI aims to divide the image space into distinct tissue classes, such as gray matter (GM), white matter (WM), and cerebrospinal fluid (CSF). The objective is to group objects within each cluster that exhibit greater similarity to each other compared to objects belonging to different clusters. This clustering process relies on a similarity or dissimilarity metric and operates without prior knowledge of the exact number of clusters [16].

Utilizing the KIFCM clustering technique serves the purpose of leveraging the advantages of Fuzzy C-means in terms of accuracy while maintaining a comparable iteration number to that of Fuzzy C-means and K-means. This approach aims to reduce the overall time consumption during program execution. The KIFCM algorithm is employed in the processing of the data for achieving the desired results. The result of KIFCM algorithm of filtered images can be observed in Fig. 3, where the filtered images are clustered into gray matter and white matter. And Algorithm 2 shows how KIFCM clustering algorithm works to Obtain white matters and gray matters clustered brain MRI image.

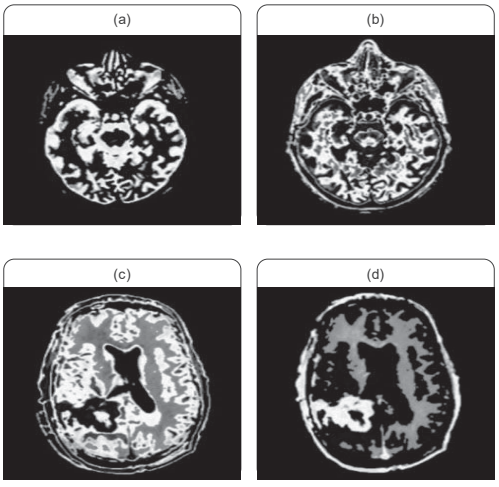

Fig. 3. This figure shows that (a and b) and (c and d) are clustered images as gray matter and white matter, respectively, after applying a hybrid algorithm (KIFCM) of filtered images

Algorithm 2 Hybrid Algorithm: KIFCM MRI Imaging Clustering

Require: Filtered brain MRI image, number of clusters (K), maximum iterations
Ensure: Obtained white matters and gray matters clustered brain MRI images
Initialize cluster centers using K-means
Initialize membership matrix and centroid matrix using FCM
Initialize iteration counter: $t = 0$
while $t <$ maximum iterations **do**
    Update membership matrix using K-means
    Update centroid matrix using FCM
    Update iteration counter: $t = t + 1$
    if Convergence criteria met **then**
        Break loop
    end if
end while
Output: Obtained white matter and gray matter clustered brain MRI images

D. Level Set Method

Following the KIFCM MRI imaging clustering step, the algorithm proceeds with the level set method for active contour segmentation. It initializes the level set function with the initial contour, iteratively updates the level set function using the active contour energy function, and evolves the level set function using the level set equation. The process continues until the convergence criteria are met or the maximum number of iterations is reached. Once the iterations are complete, the algorithm obtains the segmented regions using the final level set function. The level set function in the context of the level set method for active contour segmentation is typically represented by the symbol $\phi(x, y, t)$, where (x, y) are the spatial coordinates and t represents time.

The level set equation is used to evolve the level set function over time. One commonly used formulation is in Eq.(3) :

$$\frac{\partial \phi}{\partial t} = \alpha \cdot \text{div}\left(\frac{\nabla \phi}{|\nabla \phi|}\right) - \beta \cdot \text{dist}(x, y) \cdot |\nabla \phi| \qquad (3)$$

where, α and β are positive constants that control the evolution speed and curve smoothness, respectively. div denotes the divergence operator, and ∇ represents the gradient operator. $\text{dist}(x, y)$ represents the signed distance function that measures the distance between a point (x, y) and the contour represented by the level set function. The active contour energy functional, also known as the snake energy, is typically defined as a combination of internal and external energy terms. It can be represented as in Eq.(4):

$$\text{E}_{\text{snake}}(\phi) = \int_\Omega \left(\alpha|\nabla\phi|^2 + \beta|\nabla^2\phi|^2\right) dxdy + \int_\Omega g(x, y)|\nabla\phi|dxdy \qquad (4)$$

where, α and β are weighting coefficients that balance the influence of the internal energy terms (curvature) and the external energy term (image information), respectively. $g(x, y)$ represents the external image force that attracts the contour towards image features of interest.

Post-processing techniques can be applied, such as smoothing or morphology operations, to refine the segmented regions if necessary. Algorithm 3 shows how it works.

Algorithm 3 Level Set Method for Brain MRI Image Segmentation

Require: Clustered Brain MRI image, initial contour, maximum iterations, threshold
Ensure: Segmented regions in the brain MRI image
Initialize the level set function with the initial contour
Set the iteration counter: $t = 0$
while $t <$ maximum iterations **do**
    Update the level set function using the active contour energy functional
    Evolve the level set function using the level set equation
    Update iteration counter: $t = t + 1$
    if Convergence criteria met **then**
        Break loop
    end if
end while
Obtain the segmented regions using the final level set function
if Post-processing required **then**
    Apply post-processing techniques (e.g., smoothing, morphology operations)
end if
Output: Segmented regions in the brain MRI image

III. Results and Analysis

In this section, we conducted experiments using the proposed Method on a brain MRI image dataset. After applying our clustering algorithm on the filtered brain MRI images, we obtained the values of the initial cluster center and final cluster center of both clustered white and gray images based on the number of iterations. the results are shown in TableIII. Consequently, we conducted a performance evaluation of our proposed method by comparing it with two other algorithms, namely distributed Fuzzy C-means algorithm (DFCM) [17] and median filter with fuzzy level set (MFFLs)algorithm [18]. The comparison was based on the difference between the final cluster center and initial cluster center, considering the number of iterations for both gray matter and white matter. The results of this comparison can be found in Table II for gray matter and TableIII for white matter respectively. In order to implement active contour using the level set method, we propose the following approach. The image is divided into regions iteratively, initializing the boundaries as closed curves. These boundaries are then updated using shrink or expansion methods, taking into account the imposed constraints. The utilization of the level set method enhances flexibility, resulting in a highly efficient segmentation process that outperforms traditional techniques. Consequently, by employing the level

TABLE I. INITIAL CLUSTER CENTER AND FINAL CLUSTER CENTER OF CLUSTERED WHITE AND GRAY MATTER IMAGES BASED ON NUMBER OF ITERATIONS

Case	Number of Iterations	Sigma	Initial Cluster Center	Final Cluster Center	Time (s)
Case1	30	4	3.4781	47.8827	26.040326
Case2	200	6	9.5042	65.4276	73.80081
Case3	30	4	14.0652	79.6800	26.332371
Case4	10	4	3.0022	44.4409	4.49490

TABLE II. DFCM, MFFLS AND OUR PROPOSED METHOD COMPARISON BETWEEN FINAL CLUSTER CENTER AND INITIAL CLUSTER CENTER ON A NUMBER OF ITERATIONS FOR GRAY MATTER

Comparison	Initial cluster center		Final cluster center		Number of iterations
	Case1	Case2	Case1	Case2	
DFCM	1.1	2.5	1.100	79.667	13
MFFLs	2.0062	3.4427	88.7257	99.3391	15
Proposed method	3.4781	14.0652	47.8827	79.6800	30

TABLE III. DFCM, MFFLS AND OUR PROPOSED METHOD COMPARISON BETWEEN FINAL CLUSTER CENTER AND INITIAL CLUSTER CENTER ON A NUMBER OF ITERATIONS FOR WHITE MATTER

Comparison	Initial cluster center		Final cluster center		Number of iterations
	Case1	Case2	Case1	Case2	
DFCM	1.1	2.5	1.100	79.667	13
MFFLs	3.7634	4.1807	102.5521	103.4951	15
Proposed method	9.9565	10.7809	61.0270	44.5564	30

set method, we can accurately determine the final contour as outlined below in Fig. 4 after several iterations and with $\sigma = 4, 6$. Brain MRI images often suffer from intensity inhomogeneity due to various factors. Intensity inhomogeneity can result in uneven illumination across the image, leading to inconsistencies in the intensity values of different regions. This can make it difficult to distinguish between tumor regions and normal brain tissue accurately. According to our results, Fig. 5 shows an inhomogeneity field of both gray and white clustered images after minimizing the energy and distribution of the intensity, and followed by solving the problem to show the bais corrected of gray and white clustered images as in Fig.6.

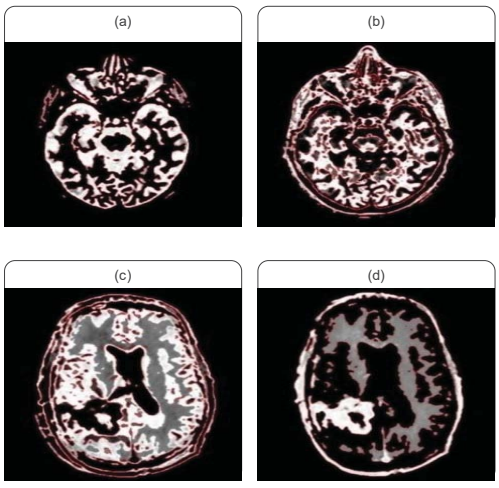

Fig. 4. This figure shows the final contour for case (a) after 30 iterations with $\sigma = 4$ and for case (b) after 200 iterations with $\sigma = 6$ and for case (c) after 30 iterations with $\sigma = 4$, and for case (d) after 10 iterations with $\sigma = 4$.

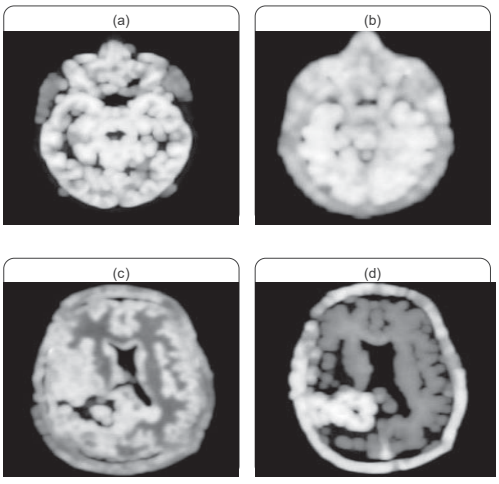

Fig. 5. This figure shows an inhomogeneity field of gray and white clustered images

IV. EVALUATION METRICS

In order to evaluate the accuracy of the performance analysis, commonly used methods are employed. These methods can be categorized into two groups: those that rely on pixel differences, such as Mean Squared Error (MSE) and Peak Signal-

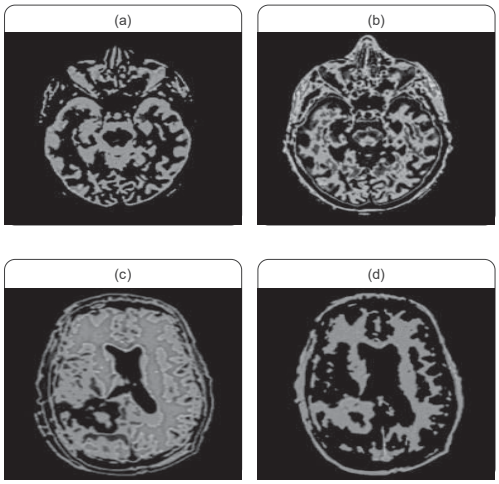

Fig. 6. Bias corrected of gray and white clustered images

to-Noise Ratio (PSNR), and those that utilize measurements based on the human visual system, such as Structural Similarity Index (SSIM). These evaluation metrics provide valuable insights into the quality and fidelity of the analyzed results. Performance analysis and accuracy parameters for FCM and K-means, including MSE, PSNR, and SSIM, are presented in Table IV. Additionally, Table V illustrates the performance analysis and accuracy parameters for the segmented images using KIFCM and FCM, respectively.

1) **Mean Squared Error (MSE):**
The Mean Squared Error (MSE) is a metric used to quantify the average squared intensity difference between the original and deformed pixels in an image. It can be calculated using Eq.(5):

$$\text{MSE} = \frac{1}{XY} \sum_{x=0}^{X-1} \sum_{y=0}^{Y-1} e(x,y)^2 \tag{5}$$

where $e(x,y)$ represents the error difference between the input and deformed images. The MSE provides a numerical value that reflects the overall discrepancy between the two images, with a lower MSE indicating higher similarity and better alignment.

2) **Peak Signal-to-Noise Ratio (PSNR):**
Signal-to-Noise Ratio (SNR) is a mathematical metric commonly employed to assess the quality of output images in comparison to their corresponding input images. SNR is determined by calculating the ratio of the signal power to the noise power, and it can be expressed using Eq.(6):

$$\text{PSNR} = 10 \log_{10} \left(\frac{s^2}{\text{MSE}} \right) \tag{6}$$

The value of s is commonly set to 255, which corresponds to an 8-bit image.

3) **Structural similarity index (SSIM):**
This method is employed to assess the quality of an image by partitioning both the input and deformed images into windows of size $n \times n$ and converting the resulting square matrices into vectors. It relies on three components: luminance (L), contrast (C), and structural (S). The calculation of this method involves the following steps:

$$\text{SSIM}(x,y) = L(x,y)^{\alpha} \cdot C(x,y)^{\beta} \cdot S(x,y)^{\gamma} \tag{7}$$

We also employed the Dice coefficient as another method to compare our proposed approach with previous methods in Table VI. The Dice coefficient was calculated for our dataset, and the summarized results are as follows: After conducting our experiments, we evaluated the accuracy performance of the proposed method by comparing it with previous studies, namely GKFCMCV [19], GKFCM-Lankaton [20], and GKFCM-FTC [21]. This comparison demonstrated the effectiveness of our results, highlighting the superior quality and accuracy achieved by our proposed approach while requiring less computational time.

TABLE IV. PERFORMANCE ANALYSIS PARAMETERS FOR SEGMENTED IMAGES USING FCM AND K-MEANS

Cases	MSE	PSNR (dB)	SSIM
Case1	0.08	59.25	0.7993
Case2	0.07	59.75	0.8080
Case3	0.04	62.50	0.7311
Case4	0.04	62.50	0.7311

TABLE V. PERFORMANCE ANALYSIS PARAMETERS FOR SEGMENTED IMAGES FOR KIFCM AND FCM.

Cases	MSE	PSNR (dB)	SSIM
Case1	0.25	66.95	0.8063
Case2	0.27	56.72	0.8786
Case3	0.26	74.96	0.8825
Case4	0.24	66.81	0.9221

TABLE VI. COMPARISON OF THE PROPOSED METHOD WITH THE FAMOUS LEVEL SET–BASED ALGORITHMS IN TERMS OF ACCURACY BASED ON DICE COEFFICIENT FOR BRAIN IMAGES.

Method	GKFCMCV	GKFCM-Lankaton	GKFCM-FTC	Proposed method
Accuracy (%) (Dice coefficient)	65	48	80	81

V. CONCLUSION

In order to address the challenge of segmenting brain MRI images with intensity inhomogeneity, we proposed a robust method. Our approach involved applying a median filter to a dataset of approximately 60 MRI images, which effectively enhanced the results by reducing artifacts. The presence of intensity inhomogeneity poses

a significant difficulty in accurately segmenting these complex tissue images. Our method aimed to prioritize both accuracy and computational efficiency. Comparative analysis with other algorithms demonstrated the excellent performance of our approach in effectively segmenting brain MRI images with intensity inhomogeneity with an accuracy of 81% that was achieved with less computational time. In the future, we aim to propose deep learning techniques to improve the quality of brain MRI image segmentation.

ACKNOWLEDGMENT

This paper is supported by Innovation Team and Talents Cultivation Program of National Administration of Traditional Chinese Medicine (No. ZYYCXTD-D-202208). Samah Abdel Aziz is grateful for financial support from CAS-TWAS Fellowship.

REFERENCES

[1] S. Gangadhar, C. Naveena, S. Poornachandra, and V. M. Aradhya, "Preprocessing of mr images for effective quantitative image analysis," in *2019 Fifth International Conference on Image Information Processing (ICIIP)*. IEEE, 2019, pp. 63–67.

[2] M. Huang, W. Yang, Y. Wu, J. Jiang, W. Chen, and Q. Feng, "Brain tumor segmentation based on local independent projection-based classification," *IEEE transactions on biomedical engineering*, vol. 61, no. 10, pp. 2633–2645, 2014.

[3] S. Padhy, S. Dash, T. Shankar, V. Rachapudi, S. Kumar, and A. Nayyar, "A hybrid crypto-compression model for secure brain mri image transmission," *Multimedia Tools and Applications*, pp. 1–21, 2023.

[4] H. M. Rai, K. Chatterjee, and A. Nayyar, "Automatic segmentation and classification of brain tumor from mr images using dwt-rbfnn," in *Advanced Soft Computing Techniques in Data Science, IoT and Cloud Computing*. Springer, 2021, pp. 215–243.

[5] B. C. Govind, *MRI made easy (for beginners)*. JAYPEE BROTHERS MEDICAL P, 2022.

[6] H. Liao, S. K. Zhou, and J. Luo, "Chapter 1 - introduction," in *Deep Network Design for Medical Image Computing*, ser. The MICCAI Society book Series, H. Liao, S. K. Zhou, and J. Luo, Eds. Academic Press, 2023, pp. 1–9. [Online]. Available: https://www.sciencedirect.com/science/article/pii/B9780128243831000083

[7] C. L. Chowdhary and D. P. Acharjya, "Segmentation and feature extraction in medical imaging: a systematic review," *Procedia Computer Science*, vol. 167, pp. 26–36, 2020.

[8] C. Hao, D. Qi, L. Yu, Q. Jing, and P. Heng, "Voxresnet: deep voxelwise residual networks for brain segmentation from 3d mr images," *NeuroImage*, vol. 170, pp. 446–455, 2018.

[9] T. K. Mudgal, A. Gupta, S. Jain, and K. Gusain, "Automated system for brain tumour detection and classification using extreme gradient boosted decision trees," in *2017 International Conference on Soft Computing and its Engineering Applications (icSoftComp)*. IEEE, 2017, pp. 1–6.

[10] M. Kadkhodaei, S. Samavi, N. Karimi, H. Mohaghegh, S. M. R. Soroushmehr, K. Ward, A. All, and K. Najarian, "Automatic segmentation of multimodal brain tumor images based on classification of super-voxels," in *2016 38th Annual International Conference of the IEEE Engineering in Medicine and Biology Society (EMBC)*. IEEE, 2016, pp. 5945–5948.

[11] A. Nayyar, L. Gadhavi, and N. Zaman, "Machine learning in healthcare: review, opportunities and challenges," *Machine Learning and the Internet of Medical Things in Healthcare*, pp. 23–45, 2021.

[12] V. Venkatesh, N. Sharma, and M. Singh, "Intensity inhomogeneity correction of mri images using inhomonet," *Computerized Medical Imaging and Graphics*, vol. 84, p. 101748, 2020.

[13] S. K. Adhikari, J. Sing, D. Basu, M. Nasipuri, and P. Saha, "Segmentation of mri brain images by incorporating intensity inhomogeneity and spatial information using probabilistic fuzzy c-means clustering algorithm," in *2012 International Conference on Communications, Devices and Intelligent Systems (CODIS)*. IEEE, 2012, pp. 129–132.

[14] L. Tan and J. Jiang, "Chapter 13 - image processing basics," in *Digital Signal Processing (Third Edition)*, third edition ed., L. Tan and J. Jiang, Eds. Academic Press, 2019, pp. 649–726. [Online]. Available: https://www.sciencedirect.com/science/article/pii/B9780128150719000130

[15] E. Arias-Castro and D. L. Donoho, "Does median filtering truly preserve edges better than linear filtering?" 2009.

[16] A. Mukhopadhyay and U. Maulik, "A multiobjective approach to mr brain image segmentation," *Applied Soft Computing*, vol. 11, no. 1, pp. 872–880, 2011.

[17] F. Z. Benchara, M. Youssfi, O. Bouattane, and H. Ouajji, "A new scalable, distributed, fuzzy c-means algorithm-based mobile agents scheme for hpc: Spmd application," *Computers*, vol. 5, no. 3, p. 14, 2016.

[18] L. Maolood, "Al-salhi, resheedi & ince (2018)," *Fuzzy Segmentation of MRI Cerebral Tissue Using Level set Alogrithm. IJIRIS:: International Journal of Innovative Research in Information Security*, vol. 5, pp. 25–35.

[19] T. F. Chan and L. A. Vese, "Active contours without edges," *IEEE Transactions on image processing*, vol. 10, no. 2, pp. 266–277, 2001.

[20] S. Lankton and A. Tannenbaum, "Localizing region-based active contours," *IEEE transactions on image processing*, vol. 17, no. 11, pp. 2029–2039, 2008.

[21] Y. Shi and W. C. Karl, "A real-time algorithm for the approximation of level-set-based curve evolution," *IEEE transactions on image processing*, vol. 17, no. 5, pp. 645–656, 2008.